

Imaging in pancreatic disease

Julien Dimastromatteo¹, Teresa Brentnall² and Kimberly A. Kelly¹

Abstract | Pancreatic diseases, chronic pancreatitis, pancreatic cancer and diabetes mellitus, taken together, occur in >10% of the world population. Pancreatic diseases, as with other diseases, benefit from early intervention and appropriate diagnosis. Although imaging technologies have given clinicians an unprecedented toolbox to aid in clinical decision-making, advances in these technologies and development of molecular-based diagnostic tools could enable physicians to identify diseases at an even earlier stage and, thereby, improve patient outcomes. In this Review, we discuss and identify gaps in the use of imaging techniques for the early detection and appropriate treatment stratification of various pancreatic diseases, including diabetes mellitus, acute and chronic pancreatitis and pancreatic cancer. Imaging techniques discussed are MRI, CT, PET and ultrasonography. Additionally, the identification of new molecular targets for imaging and the development of contrast agents that are able to give molecular information in noninvasive radionuclear imaging and ultrasonography are emerging areas of innovation that could lead to increased diagnostic accuracy and improved patient outcomes.

The pancreas has both exocrine and endocrine function, controlling digestion through secretion of digestive enzymes and through insulin and glucagon secretion, which control blood sugar levels¹. Pancreatic diseases can be associated with disruption of these functions and include acute pancreatitis, chronic pancreatitis, diabetes mellitus and, to a lesser extent, pancreatic cancer (BOX 1).

Early detection of many diseases can lead to improved outcomes by providing opportunities for treatment and/or prevention of complications. One of the main challenges concerning early detection is the ability to identify patients at high risk of developing diseases during an asymptomatic period in the pathology progression. For pancreatic cancer, this early diagnosis could lead to a better prognosis and, in the case of pancreatitis, efforts can be undertaken to withdraw offending agents such as alcohol, smoking and pancreatitis-inducing drugs (for example, azathioprine). Imaging has transformed medicine since the first medical X-ray radiography in 1895, giving clinicians unprecedented ability to ‘see’ inside the body. Conventional diagnostic imaging, such as endoscopy, CT scan, MRI, plain X-ray radiography, fluoroscopy, ultrasonography and endoscopic ultrasonography (EUS), have been used medically for diagnosis and treatment planning in a variety of pathologies (BOX 2)^{2,3}. Molecular imaging aims to use current imaging systems in combination with probes or tracers that bind to and enable detection of disease-specific molecules. As such, molecular imaging can be a complementary approach to conventional diagnostic imaging. Multimodal imaging systems such as single-photon

emission computed tomography (SPECT)–CT, PET–CT and PET–MRI combine the best of both conventional diagnostic and molecular modalities, with the high resolution and high sensitivity of molecular imaging paired with anatomical or functional information of conventional diagnostic imaging. In the following sections, we review current imaging technologies and discuss new technologies that hold the potential to transform clinical treatment and diagnosis of pancreatic diseases.

Imaging approaches

Conventional imaging

Currently, endoscopy, CT, MRI and ultrasonography form the core imaging methodologies for pancreatic diseases. Depending on the imaging modality used, the resulting images can reflect the anatomy, metabolism or molecular aspects of the tissue of interest (TABLE 1).

CT, MRI and ultrasonography are typically non-invasive imaging modalities that are widely available globally. For a thorough and complete discussion of the physics of medical imaging, we refer our readers to the textbook, *The Essential Physics of Medical Imaging*⁴. CT is a radiographic imaging system using X-rays as an energy source. Images are the result of differences in tissue density (for example, high-density bone tissue versus low-density lung tissue), which correspond to differences in absorption and scatter (so-called attenuation) of the energy⁴. The signal in MRI derives from the use of strong electromagnetic fields and the inherent magnetism of unpaired protons⁴. Owing to the large amounts of fluid (H₂O) in the body, the ¹H⁺ molecule

¹Department of Biomedical Engineering, University of Virginia, 415 Lane Road, Building MR5, Charlottesville, Virginia 22903, USA.

²Division of Gastroenterology, Digestive Diseases Center, 1959 Northeast Pacific Street, Seattle, Washington 98195, USA.

Correspondence to K.A.K. kak3x@virginia.edu

doi:10.1038/nrgastro.2016.144
Published online 9 Nov 2016

Key points

- Pancreatic cancer is frequently diagnosed after the appearance of symptoms, which is too late for curable treatment
- No blood test currently exists for chronic pancreatitis and the diagnosis can be difficult to make, even with current imaging technologies
- Treating pancreatic disease at an early stage of the pathogenesis could lead to better prognosis
- Currently used imaging techniques have various limitations, including difficulty in discriminating between benign and malignant conditions
- Molecular imaging can augment conventional imaging modalities for the diagnosis of incipient pancreatic diseases

is the most abundant proton present in the body and consequently can be used to provide contrast between tissues with various amounts of fluid content. In addition, magnetic resonance cholangiopancreatography (MRCP) is a type of MRI that uses a magnetic resonance sequence sensitive to static fluid to generate high-resolution images for the evaluation of the the biliary and pancreatic ductal system.

Ultrasonography uses high-frequency soundwaves as energy, and image generation relies on the intrinsic echo acoustic characteristics of the tissue examined⁴. Usually noninvasive, this technology is also used invasively as EUS. Contrast-enhanced ultrasonography (CEUS) and contrast-enhanced endoscopic ultrasonography (CE-EUS) use intravenous contrast agents such as inert gas-filled microparticles, termed microbubbles, that are equal to or smaller than the size of a red blood cell, to improve visualization of the macrovasculature and microvasculature during an ultrasonography assessment of organs. Use of the contrast agent provides information about vascular patterns that can assist in

disease identification⁵. The contrast agent can be used in conjunction with transabdominal ultrasonography (often used for the evaluation of the liver) or can be combined with EUS, to provide high-resolution images for the evaluation of neoplastic or inflammatory lesions in the pancreas⁶. CEUS and CE-EUS are widely used in Europe and Asia, but unfortunately contrast agents for ultrasonography have yet to be approved by the FDA for use in abdominal imaging in the USA⁷. CEUS and CE-EUS are used in the evaluation of solid and cystic pancreatic lesions, as well as in chronic and acute pancreatitis. Typically, the enhancement pattern of a focal pancreatic lesion is compared with the adjacent healthy pancreatic tissue. Adenocarcinoma tends to be hypovascular and therefore hypoenhancing, whereas neuroendocrine tumours are hyperenhancing⁸. Other features that can distinguish lesions include the wash-out period of the enhancing agent during arterial versus venous phases, location of vasculature within a lesion, rim-enhancement and cystic features⁹.

Endoscopic retrograde cholangiopancreatography (ERCP) requires endoscopy, cannulation of the entrance of the pancreatic duct with a small tube, injection of contrast reagent into the pancreatic duct and fluoroscopy of the contrast-induced images. Currently, ERCP is rarely used for diagnostic purposes, as it has been replaced by alternative imaging techniques such as EUS. Instead, ERCP is typically performed when treatment is required, such as placement of a stent in pancreatic duct strictures, and provides anatomical or structural information on the pancreatic ducts. Technological improvements to endoscopy have led to the development of confocal laser endomicroscopy (CLE), which enables the visualization of the ductal endothelial environment at a microscopic level in real time. Unfortunately, this promising technique has limited clinical utility to date because of its high cost and low availability¹⁰.

Box 1 | Key characteristics of pancreatic disease

Acute pancreatitis

- Causes: acute inflammation of the pancreas that can be caused by drug toxicity including alcohol, obstruction (such as gallstones) and trauma
- Symptoms: pain in the upper abdomen that can radiate through the back; nausea; vomiting

Chronic pancreatitis

- Causes: alcohol use; genetic causes such as cystic fibrosis; high lipid levels; autoimmune conditions and idiopathic causes
- Early-phase symptoms: recurrent episodes of pain; nausea; vomiting; transient weight loss
- Late-phase symptoms: diabetes mellitus; malabsorption; weight loss

Pancreatic cancer

- Causes: genetic predisposition in ~10% of cases; environmental risk factors include smoking, chronic inflammation of the pancreas from any cause and new-onset diabetes mellitus in adults without obesity
- Symptoms: weight loss; jaundice; indigestion; nausea; vomiting; abdominal and back pain; loose stools and/or malabsorption

Diabetes mellitus

- Causes: genetic predisposition; obesity; lack of physical activity; poor diet; underlying primary pancreatic diseases
- Symptoms: frequent urination; increased thirst; increased hunger

Molecular imaging

To augment conventional imaging, molecular imaging is crucial as it enables precise assessment among patients on the basis of molecular differences — not just structural or anatomical changes. For many diseases, detrimental molecular changes occur several years before the appearance of symptoms, a property that is especially true of diseases of the pancreas. A study based on exome sequencing analyses of resected pancreatic tumours estimated the timeline of molecular transitions from a benign to malignant state to be 20 years¹¹. This timeframe is mirrored in the metabolic and molecular changes in patients with pancreatic disease, such as insulin resistance, which precede symptomatic diabetes mellitus by 10 years¹². Given the early molecular changes in these patients, molecular imaging has the potential to provide a diagnosis of incipient disease among individuals with no obvious symptoms. Although molecular imaging is not feasible on a population-wide basis, patients who are subject to high genetic and environmental risk factors for disease or who have a positive serum test for a disease would be candidates for imaging. Much work has been done to identify circulating biomarkers of disease

Box 2 | Imaging techniques glossary

CT

Imaging procedure that uses special X-ray radiography equipment to create detailed pictures, or scans, of areas inside the body, also called computerized tomography and computerized axial tomography.

Confocal laser endomicroscopy (CLE)

Technique for obtaining real-time histology-like images from inside the human body.

Contrast-enhanced ultrasonography (CEUS)

Refers to use of intravenous contrast agents to improve visualization of the microvasculature and macrovasculature during an ultrasonographic assessment of organs.

Elastography

Imaging modality that maps the elastic properties of soft tissue.

Endoscopic retrograde cholangiopancreatography (ERCP)

Imaging procedure to visualize the pancreas or its ducts by X-ray radiography following injection of a contrast medium into the ducts at surgery via an endoscope.

Endoscopic ultrasonography (EUS)

Imaging procedure in which endoscopy is coupled with ultrasonography to visualize the internal organs.

Endoscopy

Nonsurgical procedure used to examine the digestive tract.

Fluoroscopy

Real-time X-ray radiographic imaging that is especially useful for guiding diagnostic and interventional procedures.

Laparoscopy

Surgical intervention that uses a thin, lighted tube put through an incision in the belly to look at the abdominal organs.

Magnetic resonance cholangiopancreatography (MRCP)

A noninvasive imaging technique that uses MRI to obtain images of the biliary and pancreatic ducts.

MRI

Noninvasive imaging modality that uses a powerful magnetic field, radio frequency pulses and a computer to produce detailed pictures of organs, soft tissues, bone and virtually all other internal body structures.

PET

Imaging technique that uses a radioactive substance (beta⁺ photon, also called a positron) to look for disease in the body.

Single-photon emission computed tomography (SPECT)

Imaging technique that uses a radioactive substance (gamma photon) to look for disease in the body.

Ultrasonography

Imaging modality that uses high-frequency acoustic wave to image the body. Involves the use of a small transducer (probe) and ultrasound-conductive gel placed directly on the skin.

Imaging modalities such SPECT or PET are based on the detection of gamma emission or beta-positive emission, respectively, from radioisotopes that emit high-energy photons, such as the commonly used ^{99m}Tc, ¹¹¹In and ¹²³I, for SPECT, or ¹⁸F, ⁶⁴Cu and ⁸⁹Zr, for PET. Targeted CEUS uses high-frequency sound waves in association with molecularly targeted microbubbles as a contrast agent^{18–20}. Although targeted CEUS exhibits high sensitivity, molecular targets are currently constrained to the vascular lumen as the microbubbles are unable to extravasate from the vessels into the interstitium owing to their large size. Optical imaging systems are also capable of screening at the nanomolar level of sensitivity²¹. Optical molecular imaging techniques commonly incorporate fluorescent dyes, quantum dots or gold nanoparticles conjugated to targeted carriers such as antibodies or peptides. High spatial resolution and real-time imaging are features that give optical imaging value over nuclear imaging modalities; however, a major drawback for clinical application of the optical techniques originates from the low tissue-penetration capability, as fluorescent dyes can only be detected superficially (up to 1 cm depth)²². This limitation prevents use of optical imaging when no direct access to the organ is available, as is the case in most clinical presentations. However, such techniques can be implemented to help surgeons during tumour resection procedures using fluorescent laparoscopy. Here, we review the latest and most promising disease imaging targets, probes and methods in molecular imaging of pancreatic diseases.

Imaging in pancreatic disease**Pancreatitis**

Inflammation of the pancreas occurs when pancreatic digestive enzymes attack the pancreas itself²³. The most frequent risk factors for pancreatitis are heavy alcohol use, cystic fibrosis, high lipid or calcium levels, obstruction of the pancreatic duct by gallstones or gallbladder sludge and autoimmune conditions (BOX 1)²³. The aetiology in many cases of pancreatitis is unknown and deemed idiopathic pancreatitis. Pancreatitis can be acute, recurrent or chronic depending on the frequency of occurrence. The risk of gallstone-induced pancreatitis is >2% in patients who have an asymptomatic gallstone²⁴. Frequently, acute pancreatitis symptoms reverse within a few days after administration of intravenous fluids and supportive care, whereas the chronic form generates irreversible damage and complications. Chronic pancreatitis is frequently caused by heavy alcohol use, although other causes exist, such as genetic disorders, cystic fibrosis or hereditary pancreatitis. The prevalence of chronic pancreatitis is difficult to define as long-term follow-up of people with chronic alcohol issues is problematic²⁵. However, studies performed in a population after autopsy suggest ~10% prevalence of occult disease^{26–28}. Additionally, chronic pancreatitis is a risk factor for the development of pancreatic cancer^{29,30} and can at times appear similar to pancreatic adenocarcinoma (PDAC) lesions at imaging. As a result, discrimination of an inflamed pancreas from the early stages of carcinogenesis is an ongoing challenge for clinicians³¹.

such as proteins¹³, long noncoding RNAs¹⁴, exosomes¹⁵ and circulating tumour cells¹⁶. A diagnostic strategy encompassing these 'liquid biopsy' samples followed by molecular imaging should enable much earlier detection of disease than currently possible¹⁷.

Molecular imaging requires instruments with high sensitivity that are able to detect features in the micromolar or nanomolar range (TABLE 1). When considering clinical imaging at a molecular scale, the quantity of target molecule available per tissue surface unit, that is, the target density, must be taken into account, along with the requisite high sensitivity of detection by several of the noninvasive technologies available on the market.

Table 1 | **Imaging methods in pancreatic disease**

Modality	Spatial resolution	Parameters imaged	Depth	Acquisition time	Cost per scan* (US\$)	Clinical use
PET	1–2 mm	Metabolism, immunology	No limit	Minutes or hours	\$1,000–\$2,000	Yes
SPECT	1–2 mm	Metabolism, immunology	No limit	Minutes or hours	\$1,000–\$1,500	Yes
Ultrasonography	<100 μm	Structure, metabolism	cm	Seconds or minutes	\$200–\$400	Yes
MRI	<100 μm	Structure, metabolism	No limit	Minutes or hours	\$800–\$1,200	Yes
CT	<100 μm	Structure	No limit	Minutes	\$600–\$800	Yes
FRI	1–3 mm	Metabolism, immunology	cm	Seconds or minutes	NA	No
FMT	1 mm	Metabolism, immunology	10 cm	Seconds or minutes	NA	No

*Cost per scan can vary depending on the price of the contrast agent. FMT, fluorescence-mediated molecular tomography; FRI, fluorescence reflectance imaging; NA, not commercially-available; SPECT, single-photon emission CT.

Current imaging technologies for acute pancreatitis.

According to the revised Atlanta classification, acute pancreatitis is diagnosed when two of the three following criteria are met: symptoms such as abdominal pain (often spreading to the back), high serum content of lipase or amylase and/or specific features on imaging scans such as gallstones or early duct disruption^{32,33}. In the majority of cases, pancreatic imaging is not performed at the beginning of the diagnostic process unless complications are suspected. However, in a medical emergency, ultrasonography is useful as it enables a quick initial examination of the abdominal region, and should be carried out as early in the disease course as possible. To determine the severity of the pancreatitis, morphological information is necessary and contrast-enhanced CT is the modality most often used. The sensitivity demonstrated by MRI or EUS, which provides detailed characterization of the pancreatic tissue and ducts, enables the categorization of acute pancreatitis into two groups: interstitial oedematous pancreatitis, in which the symptoms resolve within a week³⁴, and necrotizing pancreatitis, which can be more severe³⁵.

The decision to administer contrast agent in patients is always a matter of clinical judgement. Patients experiencing acute renal failure, one of the most deadly complications of acute pancreatitis³⁶, or patients presenting iodinated contrast agent allergies are contraindicated according to the American College of Gastroenterology guideline³⁷. CEUS has been used in the diagnostic evaluation of patients with pancreatitis; however, comparison of the enhancement pattern can be complicated in these patients because the extent of the disease can preclude comparisons of normal adjacent tissue. In general, inflamed pancreatic tissue is hypervascular compared with healthy pancreatic tissue, and areas of necrosis appear as nonenhancing³⁸. CEUS can be particularly valuable in the evaluation of patients with acute pancreatitis who frequently have associated renal impairment, owing to the lack of toxicity of the microbubble-based contrast agents³⁹. In such patients, contrast CT can be problematic owing to the renal toxicity resulting from the high osmolarity of iodinated products⁴⁰. CEUS has the advantage of identifying necrosis and pseudocysts, and can be used in a serial fashion without radiation exposure or renal toxicity.

One study compared 50 consecutive patients with acute pancreatitis diagnosed by CEUS versus standard CT scanning⁴¹. The sensitivity and specificity of CEUS in detecting severe acute pancreatitis was 91% and 100%, respectively, when compared to CT scanning. A statistically significant correlation was found between CT and CEUS severity index ($r=0.926$), between the extent of necrosis in CT and CEUS ($r=0.893$) and between CT and CEUS-determined Balthazar grade ($r=0.884$), which is a five-level scale based on pancreas appearance on the scan.

Current imaging technologies for chronic pancreatitis.

Chronic pancreatitis is notoriously difficult to diagnose, as the disease can be patchy and mild. For instance, 16 of 36 patients with alcoholism and no symptoms of pancreatitis showed postmortem evidence of chronic pancreatitis, including fibrosis, inflammation and loss of exocrine tissue⁴². Although testing for elevated serum lipase and amylase levels can be useful for the diagnosis of acute pancreatitis⁴³, no applicable blood test currently exists for chronic pancreatitis, and consequently this disease is diagnosed mainly through imaging. Standard imaging of chronic pancreatitis using CT scans and MRI is insensitive for identification of the early stages of the disease⁴⁴, as by the time changes in calcification and heterogeneity of the pancreas are detectable, the disease is already advanced. Conventional imaging for late disease can include CT or MRI scans. These scans can detect calcifications, ductal dilation and the enlargement or atrophy of the pancreas present in chronic pancreatitis⁴⁵. MRI can detect parenchymal calcification, but this trait is better displayed on CT than on MRI. However, in comparison with CT, MRI yields increased resolution of intraductal calcifications, which can cause pancreatic duct obstruction⁴⁵. The sensitivity and specificity of CT in detecting chronic pancreatitis is 74–90% and 85%, respectively; however, the accuracy of the imaging test usually has a positive correlation with the severity of the disease, with sensitivity increasing with severity⁴². MRCP with or without enhancement using secretin, which can be administered to stimulate fluid secretion from the main pancreatic duct, can assist in early disease diagnosis. MRCP enables high-resolution imaging of pancreatic ductal irregularities, and has the potential

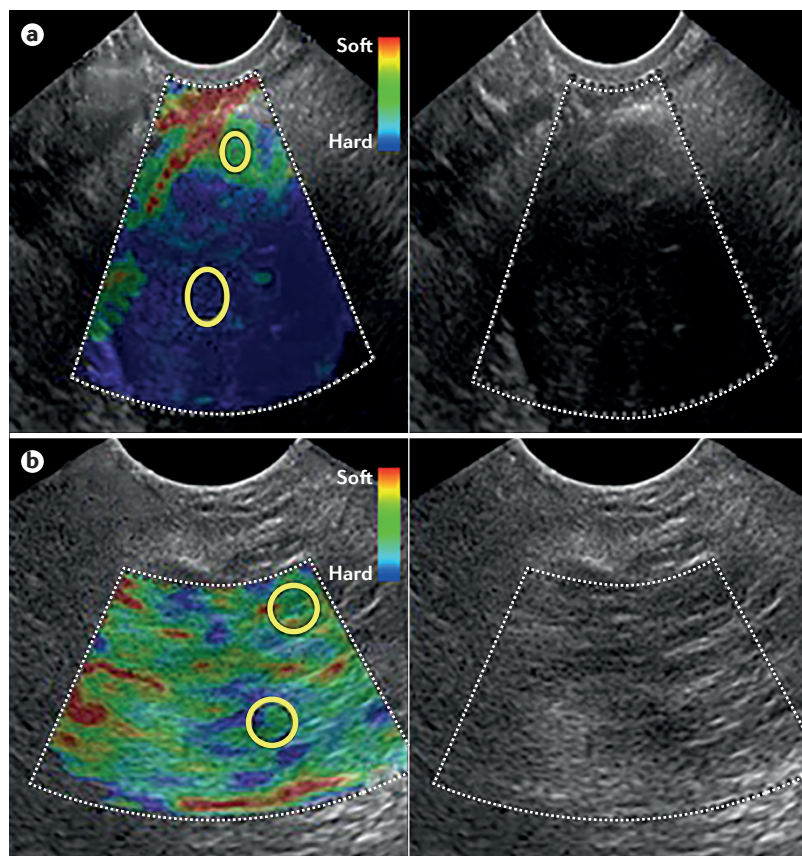


Figure 1 | Use of endoscopic ultrasonography in pancreatic lesions. Endoscopic ultrasound elastography images (left panels) result from the superimposition of tissue stiffness (colourmap) over traditional endoscopic ultrasonography images (right panels). **a** | Image obtained from a patient with a final diagnosis of adenocarcinoma. The strain ratio was 17.3. **b** | Image obtained from a patient with a final diagnosis of benign solid pancreatic lesions. The strain ratio was 2.1. Permission obtained from John Wiley and Sons © Kongkam, P. et al. *J. Gastroenterol. Hepatol.* **30**, 1683–1689 (2015).

to evaluate the degree of pancreatic exocrine insufficiency⁴⁶ as well as to detect the presence of pancreatic duct alteration⁴⁷; however, as with other imaging tests, early disease can be missed.

ERCP is usually reserved for patients who require a surgical or endoscopic intervention, such as stenting structured ducts or stone removal. ERCP offers an excellent view of the main pancreatic duct, as well as the side branches; however, a risk of developing pancreatitis exists with the procedure, the approach requires an invasive exam and the patient is subjected to radiation exposure. Consequently, ERCP is used almost exclusively for therapeutic management of the pancreas in the setting of pancreatitis with ductal abnormalities or pancreatic cancer that requires intervention⁴⁸.

Arguably, one of the best tests for diagnosing chronic pancreatitis is EUS, which provides evaluation of the pancreatic ducts and the parenchyma. Findings can include visible side-branches, cysts, lobularity, irregular ducts and stones⁴⁹. EUS remains one of the most sensitive methods for diagnosing chronic pancreatitis and EUS features in chronic pancreatitis have been codified into the Rosemont criteria for diagnosis⁵⁰. CEUS has

also been used for the diagnosis of chronic pancreatitis. Early in the course of chronic pancreatitis, the pancreatic parenchyma can appear normal or hyperechoic because of fatty infiltration and fibrosis⁵¹. With more advanced disease, heterogeneous enhancement with mixed areas of hyperechogenicity and hypoechogenicity within the same patient can be demonstrated with CEUS⁵². Other findings in chronic pancreatitis include irregular pancreatic contour, intraductal calcifications and pancreatic ductal dilatation.

One of the most promising new techniques for imaging chronic pancreatitis is EUS–elastography, which can distinguish rigidity or stiffness between tissues. The stiffness measurement of the tissues relies on sound-wave frequency variations transmitted by an echo–endoscopic probe and generates a colour map of the tissue, which enables qualitative analysis. The quotient of a soft-tissue representative area to the biggest possible region of the lesion, also called the strain ratio, enables quantification⁵³. According to clinical studies, EUS–elastography showed a diagnostic accuracy of 100% sensitivity and 93% specificity when differentiating pancreatic mass originating from inflammation or carcinogenesis⁵³ (FIG. 1). The data from a cohort of 191 patients, including 92 individuals who were diagnosed with chronic pancreatitis, were re-examined and their strain ratios computed⁵⁴. The comparison exhibited a strong correlation ($r=0.813$, $P<0.0001$) and the accuracy of EUS–elastography was 91%. EUS–elastography strain ratio has been compared with EUS–fine-needle-aspiration, with the hypothesis that elastography could resolve the false-positives generated by solid pancreatic lesions⁵⁵. However, the sensitivity of EUS–elastography by strain ratio was not superior to EUS–fine-needle-aspiration for distinguishing cancer from inflammation. Overall, despite the additional information provided, opportunities remain for developing much-needed molecular-based diagnostic tools to identify potentially cancerous lesions associated with pancreatitis.

Pancreatic cystic lesions

Pancreatic cysts can be categorized into neoplastic and non-neoplastic cysts (BOX 3). Two studies, excluding patients with known pancreatic disease, reported a prevalence of pancreatic cysts of ~2.5% of adult outpatients

Box 3 | The main pancreatic cysts and lesions

Non-neoplastic pancreatic cysts

- Pseudocyst
- Congenital cyst
- Retention cyst

Neoplastic pancreatic cysts

- Intraductal papillary mucinous neoplasm (IPMN)
- Mucinous cystic neoplasm (MCN)
- Serous cystic neoplasm (SCN)
- Solid pseudopapillary neoplasm (SPN)

Other neoplastic lesion

- Pancreatic intraepithelial lesion (PanIN)

imaged for disease unrelated to the pancreas^{56,57}. Most pancreatic cysts are considered benign, but some such as intraductal papillary mucinous neoplasm (IPMN), mucinous cystic neoplasm and solid pseudopapillary neoplasm can progress asymptotically to malignancy. IPMNs are considered tumours of the pancreatic ducts; they are composed of proliferative papillary epithelial cells and the production of mucin associated with tumorigenesis leads to cystic dilation⁵⁸. IPMNs account for 21–33% of pancreatic cysts in Western patient populations⁵⁹ and have the potential to progress to invasive carcinoma⁶⁰. Mucinous cystic neoplasms are also mucinous lesions, but in contrast to IPMNs, which are found in the pancreatic ducts, mucinous cystic neoplasms have no specific pancreatic location and account for 10–49% of the total pancreatic cysts found in the Western patient populations⁵⁹. Solid pseudopapillary neoplasms are less common than IPMNs or mucinous cystic neoplasms and their morphology is a mixture of solid and fluid with haemorrhage⁵⁹.

Current imaging technologies for pancreatic cysts. Cystic lesions of the pancreas are found incidentally on many imaging techniques of the abdomen, owing to a lack of symptoms. Many of these cysts are benign, but some have neoplastic potential, of which IPMNs are the most common. Differentiating which IPMNs require treatment, which would usually be surgical, can be a difficult task. CT and gadolinium-enhanced MRCP are the imaging modalities most commonly used for the diagnosis and surveillance of patients with suspected IPMNs. EUS shows remarkable capabilities for detecting smaller size lesions (<3 mm) that would be missed by conventional CT⁶¹, but can also over-detect what could be interpreted as nodules, which can lead to unnecessary surgery⁶². One of the largest studies to date that examined the role of CEUS in the diagnosis of pancreatic disease is the Pancreatic multicenter ultrasound study (PAMUS)⁶³. CEUS was compared with the gold standard of pathology in 1,439 patients with pancreatic lesions. For solid lesions, the sensitivity and specificity for diagnosing pancreatic adenocarcinoma were both 88%. The sensitivity and specificity for diagnosing a neuroendocrine tumour were 74% and 93%, respectively. For cystic lesions, the sensitivity for diagnosing a neoplasm was 78% and the specificity was 100%. Finally, the sensitivity and specificity for diagnosing a pseudocyst, defined as a dilated cavity resembling an epithelial cyst but not lined with epithelium, were 93% and 99%, respectively. The PAMUS study concluded that CEUS is accurate in the characterization of pancreatic lesions. In a separate study of 114 patients with cystic pancreatic lesions, CEUS was again found to have a high diagnostic sensitivity for pseudocysts (94%) but showed a lower specificity than the PAMUS study (77%)⁶⁴. The differences in these two studies could be due to operator variability, populations studied and in the instrumentation calibration or instruments used — the discrepancy highlights the importance of standardizing imaging techniques and consensus guidelines among imaging personnel. CEUS has also been compared favourably with MRI in the diagnosis of pancreatic cystic lesions; in one study of 33 patients with cystic lesions, the difference between the diagnostic accuracy of CEUS and MRI was not statistically significant in the identification of septa and nodules. Interobserver agreement had a kappa value of 0.86–0.94 (REF. 65) suggesting a near perfect agreement between these two techniques for the identification of septa and nodules. Lastly, CE-EUS has been helpful in distinguishing neoplastic cystic lesions from non-neoplastic lesions. In a study of 125 patients with cystic lesions of unclear neoplastic potential, CE-EUS was combined with endoscopic-guided fine-needle aspiration to identify neoplasia. All 56 patients with suspected cystic neoplasia showed a contrast-enhancing effect associated with a visible wall, septae or nodule, whereas only four of 69 pseudocysts or nondysplastic cystic lesions had a contrast-enhancing effect. Endoscopic-guided fine-needle aspiration could diagnose all premalignant and malignant lesions that were identified through CE-EUS. The long-term follow-up of the cohort without enhancing effect did not show any development of malignant cystic lesions⁶⁶.

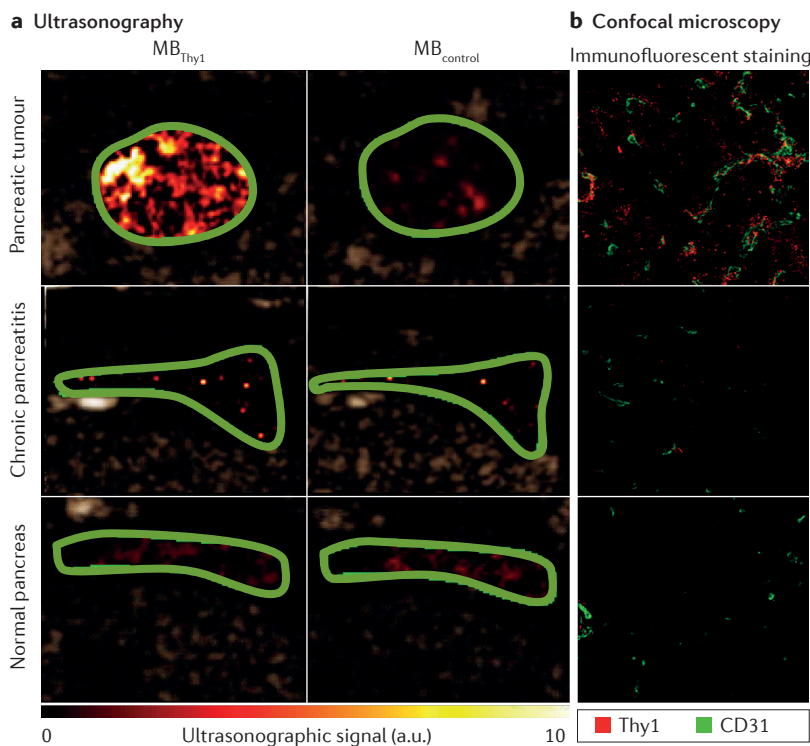


Figure 2 | Use of molecular imaging in experimental pancreatic disease. *In vivo* ultrasonographic molecular imaging of a pancreatic tumour (in a transgenic mouse model of pancreatic adenocarcinoma (top)), chronic pancreatitis (induced in mice by subcutaneous injection of L-arginine (middle)) and normal pancreas tissue (in wild-type mice (bottom)), with corresponding *ex vivo* immunofluorescence analysis²⁰. **a** | Transverse ultrasonographic images obtained in contrast mode after intravenous injection of mouse Thy1-targeted microbubbles (MB_{Thy1}) show strong imaging signal in pancreatic tumour and a low signal after injection of untargeted microbubbles (MB_{control}). Note low imaging signal after MB_{Thy1} or MB_{control} in chronic pancreatitis and normal pancreas tissue. Colour-coded scale is shown for ultrasonographic molecular imaging signal in arbitrary units (a.u.). Green lines represent regions of interest. **b** | Tiled confocal micrographs of mouse Thy1 expression. Antibodies for mouse Thy1 (red) and platelet endothelial cell adhesion molecule (CD31; green) show expression of mouse Thy1 on the tumour vasculature but no expression on the vasculature in chronic pancreatitis or in a normal pancreas. Permission obtained from Elsevier © Foygel, K. *et al. Gastroenterology* **145**, 885–894.e3 (2013).

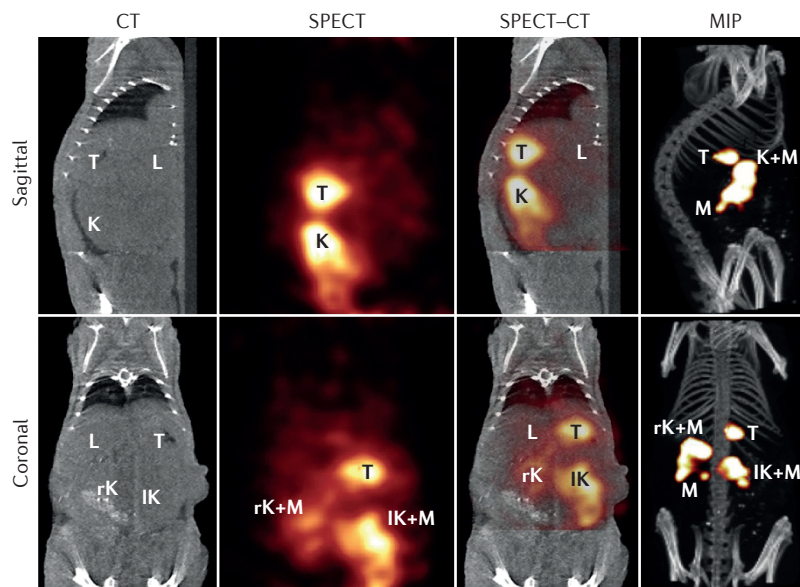


Figure 3 | Molecular imaging in a mouse model of pancreatic cancer. *In vivo* imaging of Plec in orthotopic pancreatic adenocarcinoma (PDAC) in mice. A contrast reagent that interacts with Plec was used for noninvasive *in vivo* imaging. Thymus-lacking nude mice with orthotopically implanted tumours grown from L3.6pl cells were given injections of ^{111}In -tPPT and imaged 4 h later via single-photon emission CT (SPECT) and CT. This approach showed that tetrameric plectin-targeted peptide accumulated in the PDAC, so the tumour could be imaged in the pancreas and peritoneal metastases. L, liver; IK, left kidney; M, peritoneal metastasis; MIP, maximum intensity projection; rK, right kidney; T, tumour. Permission obtained from Elsevier © Coté, G. A. et al. *Gastroenterology* **144**, 1262–1271.e1 (2013).

Confocal laser endomicroscopy has also generated improvements in diagnostic accuracy, which was increased from 53% to 86% in a population that included patients with PDAC compared with patients with a normal common bile duct⁶⁷. PET imaging using the tracer ^{18}F -fluoro-2-deoxyglucose (^{18}F -FDG) was able to differentiate benign from malignant lesions with high sensitivity (97%) and specificity (91%) compared with conventional pooled CT and MRI data with 81% sensitivity and 76% specificity, in a cohort of 467 eligible patients⁶⁸. However, cancers co-occurring with chronic pancreatitis would be missed as ^{18}F -FDG is taken up by tumours as well as inflammatory cells⁶⁹. Thus, PET tracers that are specific for cancer and malignant cysts are still needed: some examples of tracers currently under development will be highlighted in the emerging technologies section of this Review.

Precursor lesions and pancreatic cancer

Pancreatic intraepithelial neoplasms (PanINs) are the most common precursors of PDAC, the most common exocrine pancreatic cancer⁷⁰. They are categorized on the basis of their morphology and genetic modification into the following: PanIN-1A and PanIN-1B; PanIN-2; and PanIN-3 (this pancreatic progression model is discussed elsewhere⁷⁰). The detection and surgical resection of PanIN-3 lesions can potentially increase patient survival of pancreatic cancer, which has a 5-year survival of only 6%, globally⁷¹. Unfortunately, delineation between more clinically benign PanIN-1 and less benign

PanIN-3 lesions is difficult with conventional imaging techniques, and removing a PanIN-1 lesion could lead to complications such as pancreatic leak that outweigh the cancer risk⁷². New imaging approaches are required for early detection of PanIN-3s, as the number of deaths due to pancreatic cancer has surpassed those resulting from breast cancer, making pancreatic cancer the third deadliest cancer in the USA⁷³. Alarming, owing to obesity and other factors such as smoking, genetics and chronic pancreatitis, the pancreatic cancer death rate will continue to increase and is projected to be ~63,000 per year by 2030 in the USA⁷⁴, meaning that pancreatic cancer will be the number two cause of death owing to cancer by 2020 (REF. 75). PDAC symptoms occur late in disease development and are often similar to other pancreatic diseases (BOX 1); therefore, pancreatic cancer is difficult to diagnose, with most patients (~80% in the USA) being diagnosed at late stages when the disease is surgically unresectable¹⁷. Techniques for the detection of incipient pancreatic cancer are urgently needed to increase survival in this patient population.

Current imaging technologies for pancreatic cancer.

Detection of solid or cystic neoplasms usually involves CT, MRI or EUS. Abdominal CT is the most ubiquitous imaging test for detecting suspected pancreatic cancer but requires experienced radiologists to interpret images⁷⁶. Sensitivity of CT for pancreatic cancer depends on the technique used to perform the CT scan, and is highest (89–97% detection when compared with histopathology) with triple-phase or quadruple-phase, helical multidetector CT^{77,78}. Not surprisingly, the sensitivity of CT is higher for larger tumours (100% sensitivity for tumours >2 cm) than smaller tumours (77% sensitivity for tumours <2 cm)⁷⁹. As pancreatic cancer can metastasize at sizes <1 cm⁸⁰, detecting smaller lesions is of paramount importance. The typical CT appearance of a pancreatic adenocarcinoma is an ill-defined hypoattenuating mass, although smaller cancers can also be isoattenuating, making their detection difficult. Small tumours, isoattenuating cancers and tumours that subtly narrow the ductal system can be better detected by MRCP and MRI compared with CT. However, contrast-enhanced MRI and MRCP could be used interchangeably with multidetector CT depending on local practice as these modalities showed equivalent capabilities in solid tumour staging⁸¹. One of the best methods for diagnosing suspected pancreatic cancer is EUS, which offers one of the most sensitive methods for detecting smaller cancers and provides an opportunity to obtain tissue for a diagnosis, but is not available at every centre. The sensitivity for EUS combined with endoscopic-guided fine-needle aspiration exceeds 90% for detecting pancreatic cancer⁸². Importantly, the EUS abnormalities found at the earliest stages of incipient pancreatic cancer, PanIN-3, can be indistinguishable from chronic pancreatitis⁸³ when using EUS for diagnosis. For diagnosis of PDAC, EUS aids in determining the extent of disease, especially if vessel involvement is present⁸⁴. However, multidetector CT is required for full staging to determine whether local invasion

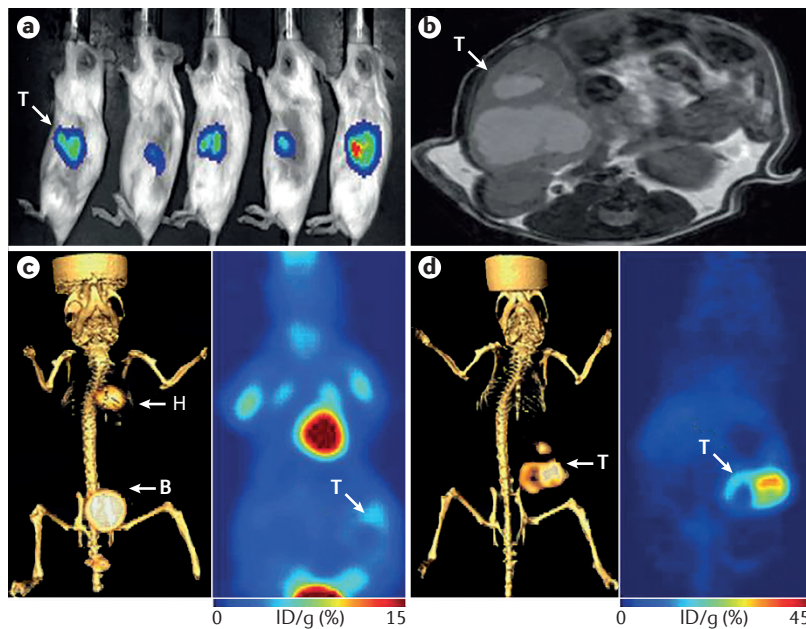


Figure 4 | PET imaging in experimental pancreatic cancer. **a** | Correlative imaging of orthotopically transplanted BxPC3 pancreatic tumour cells expressing a luciferase reporter gene. Bioluminescent optical imaging demonstrated the presence of tumours (T) in the area of surgical transplantation. **b** | MRI validated the observed tumour presence from bioluminescent optical imaging. **c** | The co-registration of ^{18}F -FDG PET and CT (left panel) and planar sections of ^{18}F -FDG PET only (right panel) displayed minimal tumour detection of the tracer with a high uptake in highly metabolic tissues: for instance, the heart (H). **d** | Acquired ^{89}Zr -5B1 PET image of the same mouse co-registered with CT exhibited exceptional tumour detection of the xenografts of BxPC3 tumour cells expressing a luciferase reporter gene. B, bladder. This research was adapted from the *Journal of Nuclear Medicine*¹¹¹. Viola-Villegas, N. T. *et al.* Applying PET to broaden the diagnostic utility of the clinically validated CA19.9 serum biomarker for oncology. *J Nucl Med* 2013; **54**:1876–1882. © by the Society of Nuclear Medicine and Molecular Imaging, Inc.

into adjacent structures or metastatic disease is present⁸⁵. To summarize, EUS and CT are complementary approaches for diagnosing and staging PDAC.

Molecular imaging of pancreatic cancer. The cellular composition of pancreatic cancers provides multiple opportunities and targets for molecular imaging. Evaluating alterations in tumour vasculature has been of particular interest to imaging researchers. Vascular endothelial growth factor receptor 2 (VEGFR2) has a major function in tumour angiogenesis. VEGFR2 is overexpressed on the neovasculature of pancreatic cancer^{86–95}, as well as in other types of cancers. VEGFR2 was detected in mouse adenocarcinoma vasculature using CEUS modality coupled with a contrast agent of VEGFR2-targeted microbubbles, supporting the feasibility of this approach for tumour detection in patients⁹⁶. Subsequently, VEGFR2 expression was monitored by CEUS in mouse subcutaneous pancreatic cancer xenograft models⁹⁷. The researchers extended their observations by using a genetically engineered mouse model of spontaneous PDAC development⁹⁸. Together, these studies have underscored the potential for stratifying patients with tumorigenesis and VEGFR2 neovasculature from those who have ongoing

inflammation with physiologically normal blood vessels that are VEGFR2 negative. In addition to VEGFR2 imaging, investigators have begun to focus on Thy1, a membrane glycoprotein that was identified as a relevant target for incipient and early-stage pancreatic cancer²⁰. Thy1-targeted microbubbles provided highly sensitive and specific contrast-enhancement for molecular ultrasonography in the detection of subcutaneous and orthotopic PDAC tumours. In a transgenic pancreatic cancer mouse model, PDAC as small as 3 mm diameter could be detected reliably (FIG. 2)²⁰.

The tumour microenvironment, or stroma, is of current interest to researchers because of its important role in carcinogenesis, progression and metastasis⁹⁹; quantitative second-harmonic-generation microscopic analysis based on variations in a specimen's ability to generate second-harmonic light from the incident light, demonstrated that desmoplastic collagen-rich PDAC stroma exhibits increased alignment, length and width of collagen fibres compared with physiologically normal and benign ducts in chronic pancreatitis¹⁰⁰. The presence of such stromal differences in the tumour microenvironment offers molecular imaging researchers a plethora of potential targets. Insulin-like growth factor I (IGF1) is known to be expressed by both stromal and tumour epithelial cells¹⁰¹. To target this expression, researchers developed IGF1-receptor-directed nanoparticles by conjugating recombinant human IGF1 antibody to magnetic iron oxide nanoparticles carrying anthracycline doxorubicin as chemotherapy¹⁰². The investigators successfully detected the orthotopic pancreatic xenograft tumours in mice using MRI and could therapeutically target the IGF1-positive tumour stroma. Similarly, SPARC, another stromal target, has been exploited for early cancer imaging using peptide-targeted nanoparticles that were elegantly discovered by phage display screening¹⁰³. The SPARC-targeted tracer was evaluated in prostate cancer, but this technology could easily be transferred to pancreatic cancer given the presence of SPARC and its involvement in PDAC progression and metastasis¹⁰⁴.

In the pursuit of targeting epithelial tumour cells, plectin, a scaffolding, cytoskeletal protein, raised considerable interest in many types of cancer, including pancreatic cancer. The specific aberrant mislocalization of plectin on the surface of PDAC epithelium contributes to its exquisite specificity for cancer and relevance as a molecular target^{105,106}. In human histopathology analysis, 60% of PanIN-3s stain positive for plectin compared with 0% in PanIN-1 and 3.9% in PanIN-2 stages. The detection of orthotopic PDAC and metastasis in nude mice lacking a thymus using ^{111}In -labelled tetrameric plectin-targeted peptide (^{111}In -tPTP)¹⁰⁷ (FIG. 3) opened the path for a phase 0 clinical trial in humans that was completed in 2016¹⁰⁸. Preliminary human data demonstrated that the agent was safe with no adverse events reported. In the three patients examined by *ex vivo* planar scintigraphy, the agent had a target-to-background accumulation ratio of >2 indicating that it was able to penetrate the tumour stroma and bind to its target on the cancer epithelial

cells. However, kidney clearance was slow, preventing *in vivo* imaging of the tumour. An enhanced version designed for rapid kidney clearance is currently being engineered¹⁰⁸.

Malignant cell transformation can lead to abnormal glycosylation. Sialyl Lewis antigen, also known as carbohydrate antigen 19-9 (CA19-9), is an epithelial leukocyte adhesion molecule and its overexpression has been correlated to carcinogenesis^{109,110}. Glycosylation, which is typically indicated in immune system response regulation, could be targeted to discriminate PDAC from chronic pancreatitis. An anti-CA19-9 human monoclonal antibody (mAb 5B1) conjugated to desferrioxamine and radiolabelled with ⁸⁹Zr (⁸⁹Zr-5B1) for PET imaging was evaluated in mouse PDAC models (FIG. 4) and showed promising results, outperforming ¹⁸F-FDG in the detection of orthotopically transplanted BxPC3 pancreatic tumour cells expressing a luciferase reporter gene¹¹¹. ⁸⁹Zr-5B1 was shown to be a potentially useful

tool in the recognition of PDAC, as it enabled visualization of tumours in mice that were serum negative for CA19-9. The same team additionally modified mAb 5B1 in a reproducible site-specific manner to be suitable for dual modality detection, PET and near-infrared fluorescence (NIRF) imaging¹¹². This dual modality technique enabled preoperative targeting of mAb 5B1 to CA19-9-positive tumours with a 100% injected dose per gramme of tissue tracer uptake, 120 h post-injection in a BxPC3 xenograft mouse model. In addition, NIRF-guided delineation of surgical margins during resection of pancreatic cancer has been successfully achieved in the same model¹¹². Unfortunately, CA19-9 can yield false-positives as a patient serum cancer biomarker, which diminishes the relevance of its use in clinical settings¹¹³. In a similar study, the overexpression of the biomarker carcinoembryonic antigen was targeted using a single chain antibody bearing NIRF dye in mice with BxPC3-derived orthotopic pancreatic xenografts¹¹⁴. The investigators showed tumour-to-background ratios as elevated as 5.1 ± 0.6 at 72 h post injection, which is suitable for intraoperative tumour delineation.

In addition to the use of antibody-based fluorescence to demarcate tumour lesions during surgical intervention, another method that involves activatable cell-penetrating peptides has been developed for *in vivo* labelling of cancer in nude mice with human cancer cell line xenografts^{115,116}. This concept takes advantage of the protease upregulation observed in most solid tumours. The construct exhibits a cleavable sequence that separates a polycationic section from a polyanionic portion. The overall neutral charge prevents the uptake of molecules by the cancer cell until proteolysis occurs. Primary pancreatic tumours were accurately visualised by labelling with ratiometric activatable cell-penetrating peptides, conjugated to Cy5 and Cy7 fluorophores, in orthotopic mouse models of human pancreatic cancer¹¹⁷. The researchers observed lower recurrence rates in the fluorescence-guided surgery group than in the white-light reflectance surgery group (38% versus 73%; $P=0.049$).

All of these studies are early in clinical development and as such, whether any of these or future agents will truly change the prognosis of the disease remains to be determined. A successful agent would be one that has >90% specificity and sensitivity for cancer over benign disease. With the advent of the exploratory Investigational New Drug mechanism of experimental drug licencing available from the FDA, imaging clinical studies have become attainable and more affordable for academic investigators, increasing the likelihood of the translation of these agents.

Diabetes mellitus

Diabetes mellitus is classified as type 1, type 2 and type 3. Type 1 diabetes mellitus refers to the alteration of insulin secretion from pancreatic β cells, whereas type 2 and type 3 diabetes mellitus refer to the resistance of insulin-sensitive organs to respond to insulin secretion. The cause of type 1 diabetes mellitus is unknown but genetic predisposition and autoimmunity have been

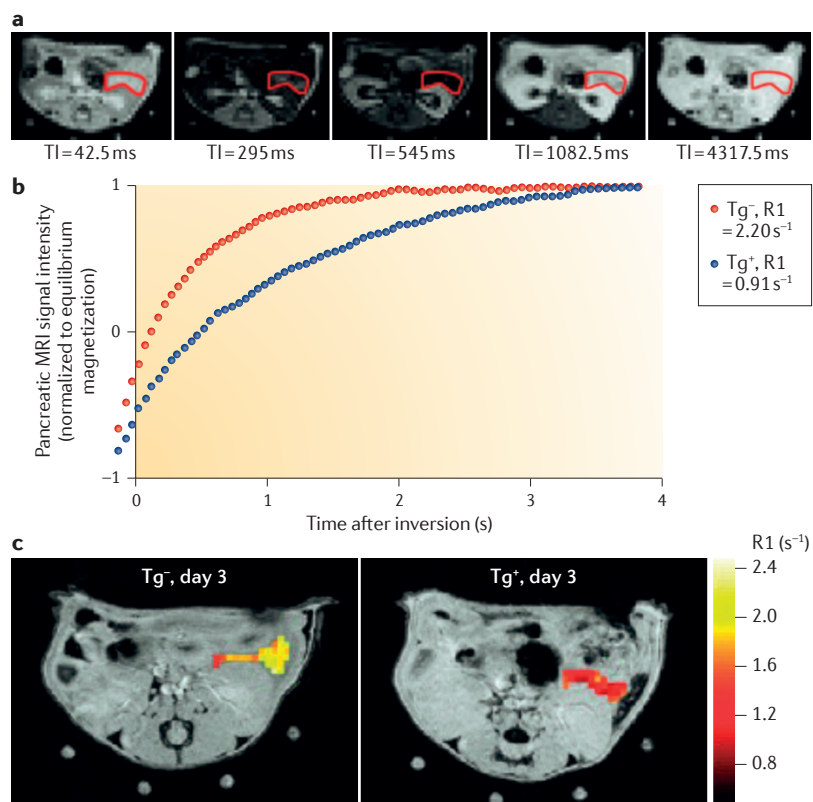


Figure 5 | Molecular imaging of experimental diabetes mellitus. a | A series of images taken using the Look-Locker method showing an axial slice through the mouse abdomen, with the pancreas outlined in red. After inversion at time 0, longitudinal magnetization returns to equilibrium with relaxation rate constant R1. The specific time after inversion (TI, in ms) is indicated below each image. **b** | Example pancreatic signal intensity versus time curves for a Tg⁻ knockout (red points) mouse and Tg⁺ knockin (blue points) mouse on day 3 after cyclophosphamide injection. Each data point on the curves represents the normalized pancreatic signal intensity measured at one TI. Pancreatic R1 was calculated by applying a monoexponential recovery model to each curve. **c** | Pixel-wise R1 maps of the pancreas from Tg⁻ (left panel) and Tg⁺ (right panel) mice on experimental day 3 overlain on high-resolution anatomic reference images. R1 is decreased in the Tg⁺ mouse at day 3 after cyclophosphamide injection. Permission obtained from American Diabetes Association © Antkowiak, P. F. *et al.* *Diabetes* 62, 44–48 (2013).

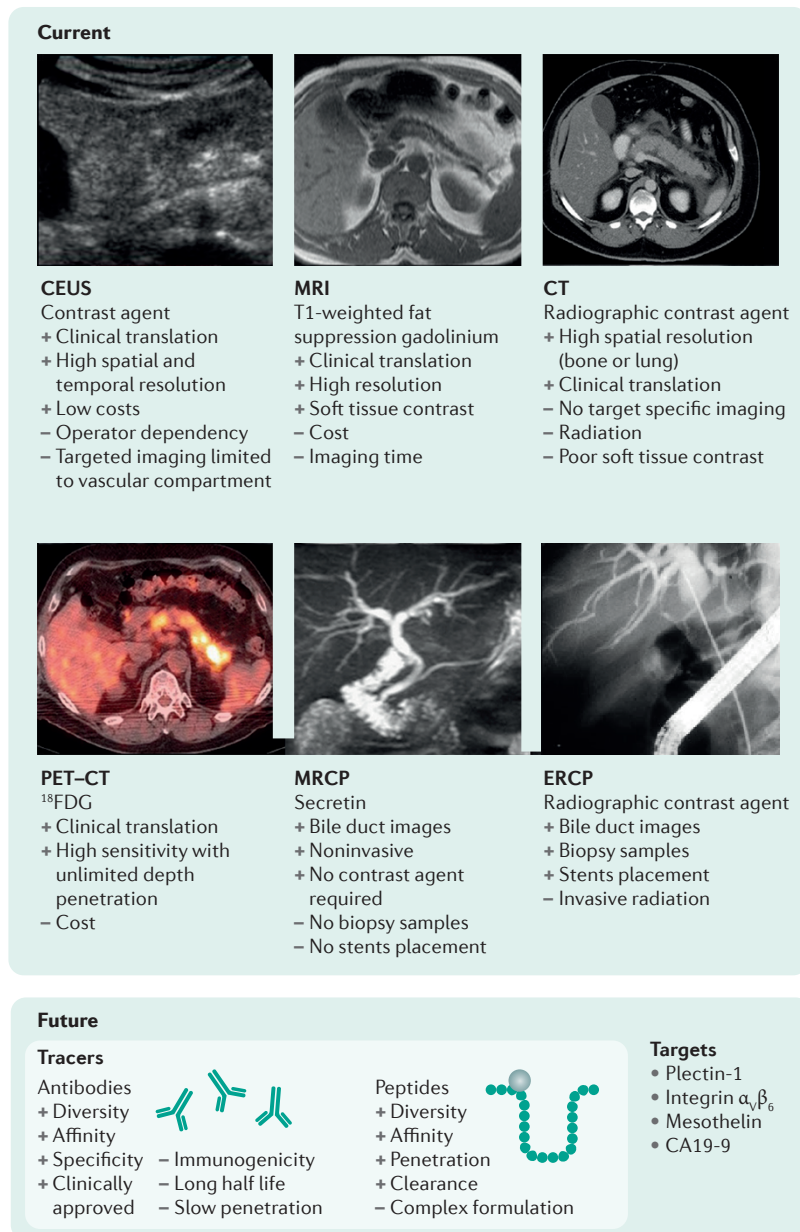


Figure 6 | Conceptual view of pancreatic disease imaging. Conventional imaging techniques such as contrast-enhanced ultrasonography (CEUS), MRI, CT, PET-CT, magnetic resonance cholangiopancreatography (MRCP) and endoscopic retrograde cholangiopancreatography (ERCP) are currently available for clinicians to aid in the diagnosis of pancreatic diseases. Molecular imaging holds considerable promise to enhance clinical decision-making and could augment current imaging approaches. Disease-specific targets such as plectin, integrin $\alpha_v\beta_6$, mesothelin or CA19-9 could give clinicians valuable molecular information that might enable earlier detection or more accurate staging of disease. Permission for CEUS image obtained from lvspring © Recaldini, C. *et al. Int. J. Med. Sci.* **9**, 203–208 (2008). MRI image adapted from Chryssou, E. G. *et al. BMC Gastroenterol.* **14**, 3:4 (2003), with kind permission from Springer Science+Business Media B.V. Permission for PET-CT image obtained from Journal of the Pancreas © Nguyen, V. X. *et al. JOP* **12**, 557–566 (2011). CT image modified from Wikimedia Commons/Hellerhoff under the Creative Commons Attribution-ShareAlike 3.0 Unported licence. To view a copy of this licence, visit <https://creativecommons.org/licenses/by-sa/3.0/>. MRCP image modified from: I. Sansoni, R. Iannaccone, R. Alcetta *et al.* (2000) Pancreas Divisum: an occasional finding. *EURORAD*. DOI: 10.1594/EURORAD/CASE.721. Permission for ERCP image obtained from American College of Gastroenterology © Domagk, D. *et al. Am. J. Gastroenterol.* **99**, 1684–1689 (2004).

implicated¹¹⁸. The risk factors for developing type 2 diabetes mellitus are mainly lifestyle related (such as diet and activity levels) and account for 90% of all diabetes mellitus cases¹¹⁹. Type 3 diabetes mellitus is caused by primary diseases of the pancreas, such as pancreatic cancer, pancreatitis or cystic fibrosis. Additionally, Alzheimer disease has been classified as type 3 diabetes mellitus as it results from a brain insuloresistance¹²⁰. In 2012, ~422 million people had diabetes mellitus (types 1–3) worldwide. This number is predicted to rise to 642 million people by the year 2040 (REF. 121).

Currently, diabetes mellitus is usually diagnosed by blood tests that measure glucose tolerance or abnormal glycosylation of haemoglobin (termed HbA_{1c})¹²². Determining the type of diabetes mellitus present can involve testing for autoantibodies, measuring exocrine pancreatic insufficiency and pancreatic imaging.

Molecular imaging of diabetes mellitus. A challenge in diabetes mellitus is the ability to assess the function and mass of pancreatic insulin-producing β cells. This difficulty occurs because of the small proportion of β cells constituting the pancreatic islets of Langerhans, representing ~2% of the total islet mass¹²³; thus, high sensitivity and spatial resolution tools are required to enable their detection.

β cells are responsible for secretion of insulin, a hormone that regulates glucose uptake in cells. Glucagon-like peptide 1 (GLP1), a 30-amino-acid peptide of the incretin family, increases secretion of insulin through activation of a GLP1 receptor (GLP1R) expressed on the β cell surface. GLP1 analogues have been used in the treatment of type 2 diabetes mellitus for decades¹²⁴ and this peptide has now also raised interest in the molecular imaging field. Several GLP1 analogues, such as exendin, have been chemically modified to generate contrast agents suitable for fluorescence imaging¹²⁵, SPECT^{126,127} or PET detection^{128,129}. A bimodal PET-fluorescence agent for imaging GLP1 expression has demonstrated encouraging preclinical results¹³⁰; ⁶⁴Cu-E4-Fl, a probe consisting of the GLP1R targeting peptide exendin-4 conjugated to a ⁶⁴Cu radiolabel and a near-infrared fluorescent dye, has been shown to delineate GLP1 receptor expression in insulinoma pancreatic endocrine tumours and pancreatic β -cell mass with high resolution. The synthesis and evaluation of similar bimodal PET-fluorescence GLP1R-targeted probes has also been reported and exhibited encouraging results as it enabled visualization of xenograft tumours with a diameter <2 mm with PET¹³¹.

β cells are also capable of incorporation of divalent cations in response to glucose stimulation¹³². This phenomenon has produced promising results in MRI. The contrast obtained by the longitudinal relaxation time (T1)-shortening of Mn²⁺ ions can efficiently differentiate diabetic from nondiabetic mice: a 50% increase in the normalized pancreas signal after glucose stimulation in nondiabetic mice was observed¹³³. Using this Mn²⁺-enhanced MRI, the same team were also able to measure gradations in β -cell mass during disease progression in a nonobese type 1 diabetes mellitus BDC2.5 T-cell

receptor transgenic mouse model after injection cyclophosphamide¹³⁴ (an alkylating cytotoxic drug known to deplete regulatory T cells¹³⁵) (FIG. 5). Within a week of the pathogenesis after cyclophosphamide injection, the investigators observed a day-to-day discriminative decrease of proton relaxation rate measured by MRI in transgene-positive mice compared with transgene-negative mice. In addition, the presence of free Zn²⁺ ions, co-released in the extracellular compartment during insulin exocytosis, has been reported as an MRI target¹³⁶. Zn²⁺ ions can be detected in T1-weighted MRI by use of a gadolinium-based Zn²⁺ sensor, GdDOTA-diBPEN. This contrast agent was sensitive enough to detect an increase in Zn²⁺ concentration reflecting neogenesis of β cells that occurred over 12 weeks of high-fat diet and observed in the progression of type 2 diabetes mellitus.

Conclusions

Diseases of the pancreas have been difficult to diagnose at early stages, and distinguishing chronic inflammatory changes of the pancreas from neoplastic change has been a challenge. Established imaging modalities such as MRI, CT, EUS, SPECT and PET are being optimized regarding data acquisition and scan analysis. In the laboratory, great effort has been made to improve the diagnostic accuracy of pancreatic disease by molecular discrimination using highly pathology-specific biomarkers. The path leading from encouraging preclinical outcomes to bedside applications is not always easy. However, through an exploitation of the molecular events that underlie these distinct diseases, emerging imaging technologies could provide valuable diagnostic tools for the clinician to augment already existing conventional imaging modalities (FIG. 6).

- Berger, H. G. *et al.* (eds) *The Pancreas* (Blackwell Publishing Ltd., 2008)
- Coté, G. A., Smith, J., Sherman, S. & Kelly, K. Technologies for imaging the normal and diseased pancreas. *Gastroenterology* **144**, 1262–1271.e1 (2013).
- Li, H., Hu, Z., Chen, J. & Guo, X. Comparison of ERCP, EUS, and ERCP combined with EUS in diagnosing pancreatic neoplasms: a systematic review and meta-analysis. *Tumour Biol.* **35**, 8867–8874 (2014).
- Bushberg, J. T. *The Essential Physics of Medical Imaging*. (Lippincott Williams & Wilkins, 2002).
- Lindner, J. R. Microbubbles in medical imaging: current applications and future directions. *Nat. Rev. Drug Discov.* **3**, 527–532 (2004).
- Rickes, S. *et al.* Contrast-enhanced sonography in pancreatic diseases. *Eur. J. Radiol.* **64**, 183–188 (2007).
- Barr, R. G. Off-label use of ultrasound contrast agents for abdominal imaging in the United States. *J. Ultrasound Med.* **32**, 7–12 (2013).
- Worhunsky, D. J. *et al.* Pancreatic neuroendocrine tumours: hypoenhancement on arterial phase computed tomography predicts biological aggressiveness. *HPB (Oxford)* **16**, 304–311 (2014).
- D'Onofrio, M., Zamboni, G., Faccioli, N., Capelli, P. & Pozzi Mucelli, R. Ultrasonography of the pancreas. 4. Contrast-enhanced imaging. *Abdom. Imaging* **32**, 171–181 (2007).
- Robles-Medrandá, C. Confocal endomicroscopy: is it time to move on? *World J. Gastrointest. Endosc.* **8**, 1–3 (2016).
- Yachida, S. *et al.* Distant metastasis occurs late during the genetic evolution of pancreatic cancer. *Nature* **467**, 1114–1117 (2010).
- Diagnosis of Diabetes and Prediabetes | National Institute of Diabetes and Digestive and Kidney Diseases (NIDDK)*. [niddk.nih.gov](https://www.niddk.nih.gov/health-information/diabetes/diagnosis-diabetes-prediabetes) Available at: <https://www.niddk.nih.gov/health-information/diabetes/diagnosis-diabetes-prediabetes> (Accessed: 7 December 2015).
- Chen, R., Pan, S., Brentnall, T. A. & Aebersold, R. Proteomic profiling of pancreatic cancer for biomarker discovery. *Mol. Cell. Proteom.* **4**, 523–533 (2005).
- Farr, R. J., Joglekar, M. V., Taylor, C. J. & Hardikar, A. A. Circulating non-coding RNAs as biomarkers of β cell death in diabetes. *Pediatr. Endocrinol. Rev.* **11**, 14–20 (2013).
- Melo, S. A. *et al.* Glypican-1 identifies cancer exosomes and detects early pancreatic cancer. *Nature* **523**, 177–182 (2015).
- Rhim, A. D. *et al.* Detection of circulating pancreas epithelial cells in patients with pancreatic cystic lesions. *Gastroenterology* **146**, 647–651 (2014).
- Chari, S. T. *et al.* Early detection of sporadic pancreatic cancer: summative review. *Pancreas* **44**, 693–712 (2015).
- Klibanov, A. L. *et al.* Targeting of ultrasound contrast material. An *in vitro* feasibility study. *Acta Radiol. Suppl.* **412**, 113–120 (1997).
- Klibanov, A. Targeted delivery of gas-filled microspheres, contrast agents for ultrasound imaging. *Adv. Drug Deliv. Rev.* **37**, 139–157 (1999).
- Foygel, K. *et al.* Detection of pancreatic ductal adenocarcinoma in mice by ultrasound imaging of thymocyte differentiation antigen 1. *Gastroenterology* **145**, 885–894.e3 (2013).
- Pogue, B. W., Leblond, F., Krishnaswamy, V. & Paulsen, K. D. Radiologic and near-infrared/optical spectroscopic imaging: where is the synergy? *AJR Am. J. Roentgenol.* **195**, 321–332 (2010).
- Rudin, M. & Weissleder, R. Molecular imaging in drug discovery and development. *Nat. Rev. Drug Discov.* **2**, 123–131 (2003).
- Whitcomb, D. C. Clinical practice. Acute pancreatitis. *N. Engl. J. Med.* **354**, 2142–2150 (2006).
- Lankisch, P. G., Apte, M. & Banks, P. A. Acute pancreatitis. *Lancet* **386**, 85–96 (2015).
- Lévy, P., Dominguez-Muñoz, E., Imrie, C., Löhr, M. & Maisonneuve, P. Epidemiology of chronic pancreatitis: burden of the disease and consequences. *United European Gastroenterol. J.* **2**, 345–354 (2014).
- Olsen, T. S. The incidence and clinical relevance of chronic inflammation in the pancreas in autopsy material. *Acta Pathol. Microbiol. Scand. A* **86A**, 361–365 (1978).
- Shimizu, M., Hayashi, T., Saitoh, Y. & Itoh, H. Interstitial fibrosis in the pancreas. *Am. J. Clin. Pathol.* **91**, 531–534 (1989).
- Stamm, B. H. Incidence and diagnostic significance of minor pathologic changes in the adult pancreas at autopsy: a systematic study of 112 autopsies in patients without known pancreatic disease. *Hum. Pathol.* **15**, 677–683 (1984).
- Whitcomb, D. C. & Pogue-Gelle, K. Pancreatitis as a risk for pancreatic cancer. *Gastroenterol. Clin. North Am.* **31**, 663–678 (2002).
- Raimondi, S., Lowenfels, A. B., Morselli-Labate, A. M., Maisonneuve, P. & Pezilli, R. Pancreatic cancer in chronic pancreatitis: aetiology, incidence, and early detection. *Best Pract. Res. Clin. Gastroenterol.* **24**, 349–358 (2010).
- Neff, C. C., Simeone, J. F., Wittenberg, J., Mueller, P. R. & Ferrucci, J. T. Inflammatory pancreatic masses. Problems in differentiating focal pancreatitis from carcinoma. *Radiology* **150**, 35–38 (1984).
- Thoeni, R. F. Imaging of acute pancreatitis. *Radiol. Clin. North Am.* **53**, 1189–1208 (2015).
- Bollen, T. L. Acute pancreatitis: international classification and nomenclature. *Clin. Radiol* **71**, 121–133 (2016).
- Singh, V. K. *et al.* An assessment of the severity of interstitial pancreatitis. *Clin. Gastroenterol. Hepatol.* **9**, 1098–1103 (2011).
- van Santvoort, H. C. *et al.* A conservative and minimally invasive approach to necrotizing pancreatitis improves outcome. *Gastroenterology* **141**, 1254–1263 (2011).
- Ljutić, D., Piplovic-Vuković, T., Raos, V. & Andrews, P. Acute renal failure as a complication of acute pancreatitis. *Ren. Fail.* **18**, 629–633 (1996).
- Tenner, S., Bailie, J., DeWitt, J., Vege, S. S. & American College of Gastroenterology American College of Gastroenterology guideline: management of acute pancreatitis. *Am. J. Gastroenterol.* **108**, 1400–1415, 1416 (2013).
- Golea, A., Badea, R., Socaciu, M., Diaconu, B. & Iacob, D. Quantitative analysis of tissue perfusion using contrast-enhanced transabdominal ultrasound (CEUS) in the evaluation of the severity of acute pancreatitis. *Med. Ultrason.* **12**, 198–204 (2010).
- Siracusano, S. *et al.* The current role of contrast-enhanced ultrasound (CEUS) imaging in the evaluation of renal pathology. *World J. Urol.* **29**, 633–638 (2011).
- Hasebroock, K. M. & Serkova, N. J. Toxicity of MRI and CT contrast agents. *Expert Opin. Drug Metab. Toxicol.* **5**, 403–416 (2009).
- Ripollés, T., Martínez, M. J., López, E., Castelló, I. & Delgado, F. Contrast-enhanced ultrasound in the staging of acute pancreatitis. *Eur. Radiol.* **20**, 2518–2523 (2010).
- Steer, M. L., Waxman, I. & Freedman, S. Chronic pancreatitis. *N. Engl. J. Med.* **332**, 1482–1490 (1995).
- Gumaste, V. V., Ruditin, N., Mehta, D. & Dave, P. B. Serum lipase levels in nonpancreatic abdominal pain versus acute pancreatitis. *Am. J. Gastroenterol.* **88**, 2051–2055 (1993).
- Chouhri, N. E., Balci, N. C., Alkaade, S. & Burton, F. R. Advanced imaging of chronic pancreatitis. *Curr. Gastroenterol. Rep.* **12**, 114–120 (2010).
- Siddiqi, A. J. & Miller, F. Chronic pancreatitis: ultrasound, computed tomography, and magnetic resonance imaging features. *Semin. Ultrasound CT MRI* **28**, 384–394 (2007).
- Bali, M. A. *et al.* Quantification of pancreatic exocrine function with secretin-enhanced magnetic resonance cholangiopancreatography: normal values and short-term effects of pancreatic duct drainage procedures in chronic pancreatitis. Initial results. *Eur. Radiol.* **15**, 2110–2121 (2005).
- Calulli, L. *et al.* Exocrine pancreatic function assessed by secretin cholangio-Wirsung magnetic resonance imaging. *Hepatobiliary Pancreat. Dis. Int.* **7**, 192–195 (2008).
- Bor, R., Madácsy, L., Fábian, A., Szepes, A. & Szepes, Z. Endoscopic retrograde pancreatography: when should we do it? *World J. Gastrointest. Endosc.* **7**, 1023–1031 (2015).
- Zuccaro, G. & Sivak, M. V. Endoscopic ultrasonography in the diagnosis of chronic pancreatitis. *Endoscopy* **24** (Suppl. 1), 347–349 (1992).
- Catalano, M. F. *et al.* EUS-based criteria for the diagnosis of chronic pancreatitis: the Rosemont classification. *Gastrointest. Endosc.* **69**, 1251–1261 (2009).
- Gardner, T. B. & Levy, M. J. EUS diagnosis of chronic pancreatitis. *Gastrointest. Endosc.* **71**, 1280–1289 (2010).
- Azemoto, N. *et al.* Utility of contrast-enhanced transabdominal ultrasonography to diagnose early chronic pancreatitis. *Biomed. Res. Int.* **2015**, 393124 (2015).
- Iglesias-García, J., Lariño-Noia, J., Abdulkader, I., Forteza, J. & Dominguez-Muñoz, J. E. Quantitative endoscopic ultrasound elastography: an accurate method for the differentiation of solid pancreatic masses. *Gastroenterology* **139**, 1172–1180 (2010).

54. Iglesias-García, J., Dominguez-Muñoz, J. E., Castiñeira-Alvarino, M., Luaces Regueira, M. & Lariño-Noia, J. Quantitative elastography associated with endoscopic ultrasound for the diagnosis of chronic pancreatitis. *Endoscopy* **45**, 781–788 (2013).
55. Kongkam, P. *et al.* Combination of EUS-FNA and elastography (strain ratio) to exclude malignant solid pancreatic lesions: a prospective single-blinded study. *J. Gastroenterol. Hepatol.* **30**, 1683–1689 (2015).
56. de Jong, K. *et al.* High prevalence of pancreatic cysts detected by screening magnetic resonance imaging examinations. *Clin. Gastroenterol. Hepatol.* **8**, 806–811 (2010).
57. Laffan, T. A. *et al.* Prevalence of unsuspected pancreatic cysts on MDCT. *AJR Am. J. Roentgenol.* **191**, 802–807 (2008).
58. Brugge, W. R., Lauwers, G. Y., Sahani, D., Fernández-del, C. C. & Warshaw, A. L. Cystic neoplasms of the pancreas. *N. Engl. J. Med.* **351**, 1218–1226 (2004).
59. de Jong, K., Bruno, M. J. & Fockens, P. Epidemiology, diagnosis, and management of cystic lesions of the pancreas. *Gastroenterol. Res. Pract.* **2012**, 147465 (2012).
60. Grützmann, R., Niedergethmann, M., Pilarsky, C., Klöppel, G. & Saeger, H. D. Intraductal papillary mucinous tumors of the pancreas: biology, diagnosis, and treatment. *Oncologist* **15**, 1294–1309 (2010).
61. Adimoolam, V. *et al.* Endoscopic ultrasound identifies synchronous pancreas cystic lesions not seen on initial cross-sectional imaging. *Pancreas* **40**, 1070–1072 (2011).
62. Anand, N., Sampath, K. & Wu, B. U. Cyst features and risk of malignancy in intraductal papillary mucinous neoplasms of the pancreas: a meta-analysis. *Clin. Gastroenterol. Hepatol.* **11**, 913–921; quiz e59–e60 (2013).
63. D'Onofrio, M. *et al.* Pancreatic multicenter ultrasound study (PAMUS). *Eur. J. Radiol.* **81**, 630–638 (2012).
64. Beyer-Enke, S. A., Hocke, M., Ignee, A., Braden, B. & Dietrich, C. F. Contrast enhanced transabdominal ultrasound in the characterisation of pancreatic lesions with cystic appearance. *JOP* **11**, 427–433 (2010).
65. D'Onofrio, M. *et al.* Comparison of contrast-enhanced sonography and MRI in displaying anatomic features of cystic pancreatic masses. *AJR Am. J. Roentgenol.* **189**, 1435–1442 (2007).
66. Hocke, M., Cui, X.-W., Domagk, D., Ignee, A. & Dietrich, C. F. Pancreatic cystic lesions: the value of contrast-enhanced endoscopic ultrasound to influence the clinical pathway. *Endosc. Ultrasound* **3**, 123–130 (2014).
67. Giovannini, M. *et al.* Results of a phase I-II study on intraductal confocal microscopy (IDCM) in patients with common bile duct (CBD) stenosis. *Surg. Endosc.* **25**, 2247–2253 (2011).
68. Sultana, A. *et al.* What is the best way to identify malignant transformation within pancreatic IPMN: a systematic review and meta-analysis. *Clin. Transl. Gastroenterol.* **6**, e130 (2015).
69. Kim, S.-L. *et al.* The effect of PPAR- γ agonist on ¹⁸F-FDG uptake in tumor and macrophages and tumor cells. *Nucl. Med. Biol.* **36**, 427–433 (2009).
70. Cornish, T. C. & Hruban, R. H. Pancreatic intraepithelial neoplasia. *Surg. Pathol. Clin.* **4**, 523–535 (2011).
71. Jemal, A., Siegel, R., Xu, J. & Ward, E. Cancer statistics, 2010. *CA Cancer J. Clin.* **60**, 277–300 (2010).
72. Allen, P. J. & Brennan, M. F. A. Selective approach to resection of cystic lesions of the pancreas: results from 539 consecutive patients. *Ann. Surg.* **245**, 825–826 (2007).
73. Pancreatic Cancer Action Network. Pancreatic Cancer Facts 2016 [online], <https://www.pancreas.org/wp-content/uploads/2016/02/2016-GAA-PC-Facts.pdf> (2016).
74. Rahib, L. *et al.* Projecting cancer incidence and deaths to 2030: the unexpected burden of thyroid, liver, and pancreas cancers in the United States. *Cancer Res.* **74**, 2913–2921 (2014).
75. National Cancer Institute SEER stat fact sheets: pancreatic cancer. <http://seer.cancer.gov/statfacts/html/pancreas.html> (2015).
76. Al-Hawary, M. M., Francis, I. R. & Anderson, M. A. Pancreatic solid and cystic neoplasms: diagnostic evaluation and intervention. *Radiol. Clin. North Am.* **53**, 1037–1048 (2015).
77. Valls, C. *et al.* Dual-phase helical CT of pancreatic adenocarcinoma: assessment of resectability before surgery. *AJR Am. J. Roentgenol.* **178**, 821–826 (2002).
78. Lee, E. S. & Lee, J. M. Imaging diagnosis of pancreatic cancer: a state-of-the-art review. *World J. Gastroenterol.* **20**, 7864–7877 (2014).
79. Bronstein, Y. L. *et al.* Detection of small pancreatic tumors with multiphasic helical CT. *AJR Am. J. Roentgenol.* **182**, 619–623 (2004).
80. Tsunoda, T. *et al.* Staging and treatment for patients with pancreatic cancer. How small is an early pancreatic cancer? *J. Hepatobiliary Pancreat. Surg.* **5**, 128–132 (1998).
81. Sahani, D. V., Shah, Z. K., Catalano, O. A., Boland, G. W. & Brugge, W. R. Radiology of pancreatic adenocarcinoma: current status of imaging. *J. Gastroenterol. Hepatol.* **23**, 23–33 (2008).
82. Harewood, G. C. & Wiersema, M. J. Endosonography-guided fine needle aspiration biopsy in the evaluation of pancreatic masses. *Am. J. Gastroenterol.* **97**, 1386–1391 (2002).
83. Templeton, A. W. & Brentnall, T. A. Screening and surgical outcomes of familial pancreatic cancer. *Surg. Clin. North Am.* **93**, 629–645 (2013).
84. Helmstaedter, L. & Riemann, J. F. Pancreatic cancer—EUS and early diagnosis. *Langenbecks Arch. Surg.* **393**, 925–927 (2008).
85. Pietryga, J. A. & Morgan, D. E. Imaging preoperatively for pancreatic adenocarcinoma. *J. Gastrointest. Oncol.* **6**, 343–357 (2015).
86. Hicklin, D. J. & Ellis, L. M. Role of the vascular endothelial growth factor pathway in tumor growth and angiogenesis. *J. Clin. Oncol.* **23**, 1011–1027 (2005).
87. Longo, R., Cacciamenti, F., Naso, G. & Gasparini, G. Pancreatic cancer: from molecular signature to target therapy. *Crit. Rev. Oncol. Hematol.* **68**, 197–211 (2008).
88. Korc, M. Pathways for aberrant angiogenesis in pancreatic cancer. *Mol. Cancer* **2**, 8 (2003).
89. Tonra, J. R. *et al.* Synergistic antitumor effects of combined epidermal growth factor receptor and vascular endothelial growth factor receptor-2 targeted therapy. *Clin. Cancer Res.* **12**, 2197–2207 (2006).
90. Spano, J.-P. *et al.* Efficacy of gemcitabine plus axitinib compared with gemcitabine alone in patients with advanced pancreatic cancer: an open-label randomised phase II study. *Lancet* **371**, 2101–2108 (2008).
91. Itakura, J. *et al.* Enhanced expression of vascular endothelial growth factor in human pancreatic cancer correlates with local disease progression. *Clin. Cancer Res.* **3**, 1309–1316 (1997).
92. Büchler, P. *et al.* Target therapy using a small molecule inhibitor against angiogenic receptors in pancreatic cancer. *Neoplasia* **9**, 119–127 (2007).
93. Higgins, K. J., Abdelrahim, M., Liu, S., Yoon, K. & Safe, S. Regulation of vascular endothelial growth factor receptor-2 expression in pancreatic cancer cells by Sp proteins. *Biochem. Biophys. Res. Commun.* **345**, 292–301 (2006).
94. Luo, J. *et al.* Pancreatic cancer cell-derived vascular endothelial growth factor is biologically active *in vitro* and enhances tumorigenicity *in vivo*. *Int. J. Cancer* **92**, 361–369 (2001).
95. Shi, Q. *et al.* Constitutive Sp1 activity is essential for differential constitutive expression of vascular endothelial growth factor in human pancreatic adenocarcinoma. *Cancer Res.* **61**, 4143–4154 (2001).
96. Korpanty, G., Carbon, J. G., Grayburn, P. A., Fleming, J. B. & Brekken, R. A. Monitoring response to anticancer therapy by targeting microbubbles to tumor vasculature. *Clin. Cancer Res.* **13**, 323–330 (2007).
97. Deshpande, N., Ren, Y., Foygel, K., Rosenberg, J. & Willmann, J. K. Tumor angiogenic marker expression levels during tumor growth: longitudinal assessment with molecularly targeted microbubbles and US imaging. *Radiology* **258**, 804–811 (2011).
98. Pysz, M. A. *et al.* Vascular endothelial growth factor receptor type 2-targeted contrast-enhanced US of pancreatic cancer neovasculature in a genetically engineered mouse model: potential for earlier detection. *Radiology* **274**, 790–799 (2015).
99. Quail, D. F. & Joyce, J. A. Microenvironmental regulation of tumor progression and metastasis. *Nat. Med.* **19**, 1423–1437 (2013).
100. Drifka, C. R. *et al.* Periductal stromal collagen topology of pancreatic ductal adenocarcinoma differs from that of normal and chronic pancreatitis. *Mod. Pathol.* **28**, 1470–1480 (2015).
101. Ouban, A., Muraca, P., Yeatman, T. & Coppola, D. Expression and distribution of insulin-like growth factor-1 receptor in human carcinomas. *Hum. Pathol.* **34**, 803–808 (2003).
102. Zhou, H. *et al.* IGF1 receptor targeted theranostic nanoparticles for targeted and image-guided therapy of pancreatic cancer. *ACS Nano* **9**, 7976–7991 (2015).
103. Thomas, S. *et al.* Development of secreted protein and acidic and rich in cysteine (SPARC) targeted nanoparticles for the prognostic molecular imaging of metastatic prostate cancer. *J. Nanomed. Nanotechnol.* **2**, <http://dx.doi.org/10.4172/2157-7439.1000112> (2011).
104. Neuzillet, C. *et al.* Stromal expression of SPARC in pancreatic adenocarcinoma. *Cancer Metastasis Rev.* **32**, 585–602 (2013).
105. Kelly, K. A. *et al.* Targeted nanoparticles for imaging incipient pancreatic ductal adenocarcinoma. *PLoS Med.* **5**, e85 (2008).
106. Shin, S. J. *et al.* Unexpected gain of function for the scaffolding protein plectin due to mislocalization in pancreatic cancer. *Proc. Natl Acad. Sci. USA* **110**, 19414–19419 (2013).
107. Bausch, D. *et al.* Plectin-1 as a novel biomarker for pancreatic cancer. *Clin. Cancer Res.* **17**, 302–309 (2011).
108. US National Library of Medicine. *ClinicalTrials.gov*, <https://clinicaltrials.gov/ct2/show/NCT01962909> (2013).
109. Kannagi, R., Izawa, M., Koike, T., Miyazaki, K. & Kimura, N. Carbohydrate-mediated cell adhesion in cancer metastasis and angiogenesis. *Cancer Sci.* **95**, 377–384 (2004).
110. Dimastromatteo, J., Houghton, J. L., Lewis, J. S. & Kelly, K. A. Challenges of pancreatic cancer. *Cancer J.* **21**, 188–193 (2015).
111. Viola-Villegas, N. T. *et al.* Applying PET to broaden the diagnostic utility of the clinically validated CA19.9 serum biomarker for oncology. *J. Nucl. Med.* **54**, 1876–1882 (2013).
112. Houghton, J. L. *et al.* Site-specifically labeled CA19.9-targeted immunoconjugates for the PET, NIRF, and multimodal PET/NIRF imaging of pancreatic cancer. *Proc. Natl Acad. Sci. USA* **112**, 15850–15855 (2015).
113. Bünger, S., Laubert, T., Roblick, U. J. & Habermann, J. K. Serum biomarkers for improved diagnostic of pancreatic cancer: a current overview. *J. Cancer Res. Clin. Oncol.* **137**, 375–389 (2011).
114. Boonstra, M. C. *et al.* Preclinical evaluation of a novel CEA-targeting near-infrared fluorescent tracer delineating colorectal and pancreatic tumors. *Int. J. Cancer* **137**, 1910–1920 (2015).
115. Jiang, T. *et al.* Tumor imaging by means of proteolytic activation of cell-penetrating peptides. *Proc. Natl Acad. Sci. USA* **101**, 17867–17872 (2004).
116. Nguyen, Q. T. *et al.* Surgery with molecular fluorescence imaging using activatable cell-penetrating peptides decreases residual cancer and improves survival. *Proc. Natl Acad. Sci. USA* **107**, 4317–4322 (2010).
117. Metildi, C. A. *et al.* Ratiometric activatable cell-penetrating peptides label pancreatic cancer, enabling fluorescence-guided surgery, which reduces metastases and recurrence in orthotopic mouse models. *Ann. Surg. Oncol.* **22**, 2082–2087 (2014).
118. Pociot, F. & Lernmark, Å. Genetic risk factors for type 1 diabetes. *Lancet* **387**, 2351–2359 (2016).
119. Ribaric, S. The rationale for insulin therapy in Alzheimer's disease. *Molecules* **21**, E689 (2016).
120. de la Monte, S. M. & Wands, J. R. Alzheimer's disease is type 3 diabetes-evidence reviewed. *J. Diabetes Sci. Technol.* **2**, 1101–1113 (2008).
121. Diabetes Atlas *DiabetesAtlas.org* <http://www.diabetesatlas.org/> (2016).
122. Kim, D. L., Kim, S. D., Kim, S. K., Park, S. & Song, K. H. Is an oral glucose tolerance test still valid for diagnosing diabetes mellitus? *Diabetes Metab. J.* **40**, 118–128 (2016).
123. Rahier, J., Guiot, Y., Goebbels, R. M., Sempoux, C. & Henquin, J. C. Pancreatic β -cell mass in European subjects with type 2 diabetes. *Diabetes Obes. Metab.* **10**, 32–42 (2008).
124. Perry, T. & Greig, N. H. The glucagon-like peptides: a double-edged therapeutic sword? *Trends Pharmacol. Sci.* **24**, 377–383 (2003).
125. Reiner, T. *et al.* Accurate measurement of pancreatic islet β -cell mass using a second-generation fluorescent extendin-4 analog. *Proc. Natl Acad. Sci. USA* **108**, 12815–12820 (2011).

126. Wild, D. *et al.* [Lys⁴⁰(Ahx-DTPA-¹¹¹In)NH₂]exendin-4, a very promising ligand for glucagon-like peptide-1 (GLP-1) receptor targeting. *J. Nucl. Med.* **47**, 2025–2033 (2006).
127. Wicki, A. *et al.* [Lys⁴⁰(Ahx-DTPA-¹¹¹In)NH₂]exendin-4 is a highly efficient radiotherapeutic for glucagon-like peptide-1 receptor-targeted therapy for insulinoma. *Clin. Cancer Res.* **13**, 3696–3705 (2007).
128. Wu, Z. *et al.* *In vivo* imaging of transplanted islets with ⁶⁴Cu-DO3A-VS-Cys⁴⁰-Exendin-4 by targeting GLP-1 receptor. *Bioconjug. Chem.* **22**, 1587–1594 (2011).
129. Connolly, B. M. *et al.* *Ex vivo* imaging of pancreatic β cells using a radiolabeled GLP-1 receptor agonist. *Mol. Imaging Biol.* **14**, 79–87 (2012).
130. Brand, C. *et al.* *In vivo* imaging of GLP-1R with a targeted bimodal PET/fluorescence imaging agent. *Bioconjug. Chem.* **25**, 1323–1330 (2014).
131. Behnam Azad, B. *et al.* Synthesis and evaluation of optical and PET GLP-1 peptide analogues for GLP-1R imaging. *Mol. Imaging* **14**, 1–16 (2015).
132. Henquin, J.-C., Nenquin, M., Stiernet, P. & Ahren, B. *In vivo* and *in vitro* glucose-induced biphasic insulin secretion in the mouse: pattern and role of cytoplasmic Ca²⁺ and amplification signals in β -cells. *Diabetes* **55**, 441–451 (2006).
133. Antkowiak, P. F. *et al.* Noninvasive assessment of pancreatic β -cell function *in vivo* with manganese-enhanced magnetic resonance imaging. *Am. J. Physiol. Endocrinol. Metab.* **296**, E573–E578 (2009).
134. Antkowiak, P. F., Stevens, B. K., Nunemaker, C. S., McDuffie, M. & Epstein, F. H. Manganese-enhanced magnetic resonance imaging detects declining pancreatic β -cell mass in a cyclophosphamide-accelerated mouse model of type 1 diabetes. *Diabetes* **62**, 44–48 (2013).
135. Ablamunits, V., Quintana, F., Reshef, T., Elias, D. & Cohen, I. R. Acceleration of autoimmune diabetes by cyclophosphamide is associated with an enhanced IFN- γ secretion pathway. *J. Autoimmun.* **13**, 383–392 (1999).
136. Lubag, A. J. M., De Leon-Rodriguez, L. M., Burgess, S. C. & Sherry, A. D. Noninvasive MRI of β -cell function using a Zn²⁺-responsive contrast agent. *Proc. Natl Acad. Sci. USA* **108**, 18400–18405 (2011).

Acknowledgements

The authors thank S. L. Hasbrouck, Curry School of Education, University of Virginia, for her kind help reading and editing the manuscript.

Author contributions

All authors contributed equally to the article.

Competing interests statement

The authors declare no competing interests.